TRIUMF

Recent results from the mass spectrometer EMMA at TRIUMF

Louis Wagner

Postdoc for DRAGON and EMMA at TRIUMF

2023 TRIUMF Science Week Jul. 31st, 2023
Vancouver, B.C. Canada

2023-08-01

Discovery, accelerated

TRIUMF ISAC Facility

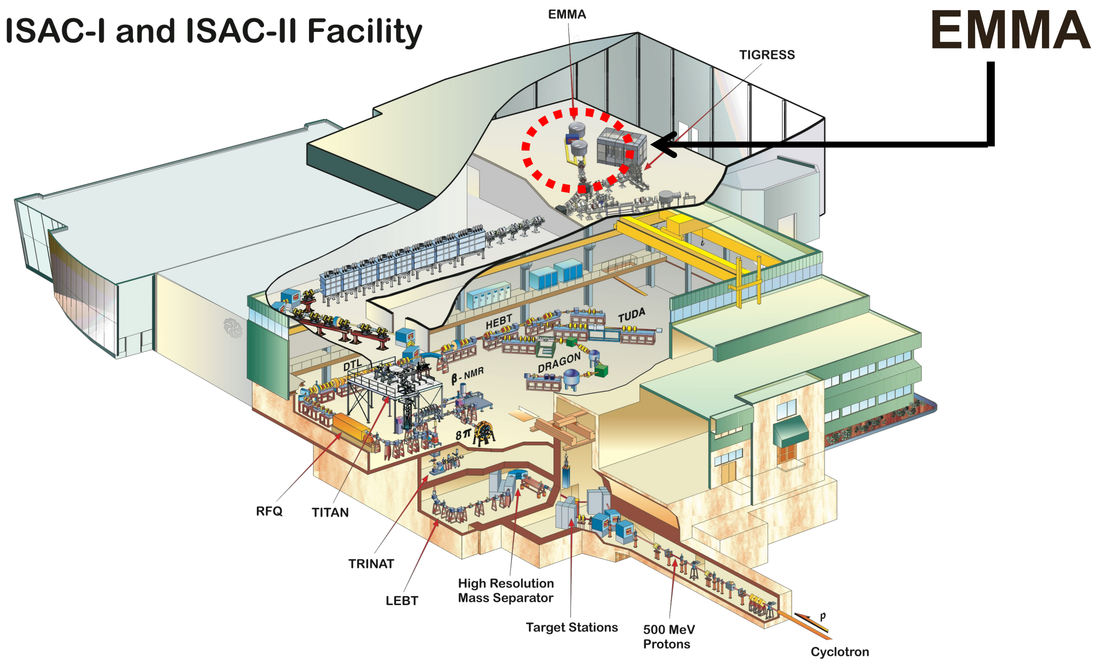

- The Isotope Separator and Accelerator (ISAC) facility at TRIUMF provides a wide variety of intense beams of exotic nuclei produced using the ISOL method
- Beams reaccelerated through 35 MHz RFQ with A/q<30
- 105 MHz variable energy DTL (3 ≤ A/q ≤ 6)
- Energies between 0.15 MeV/u & 1.8 MeV/u
- Low-energy regime well suited for reaction studies for novae & X-ray bursts
- ISAC-II SC-LINAC max. beam energies 6.5 – 16.5 MeV/u suited for transfer reactions on heavy ions

Recoil Mass Spectrometer EMMA

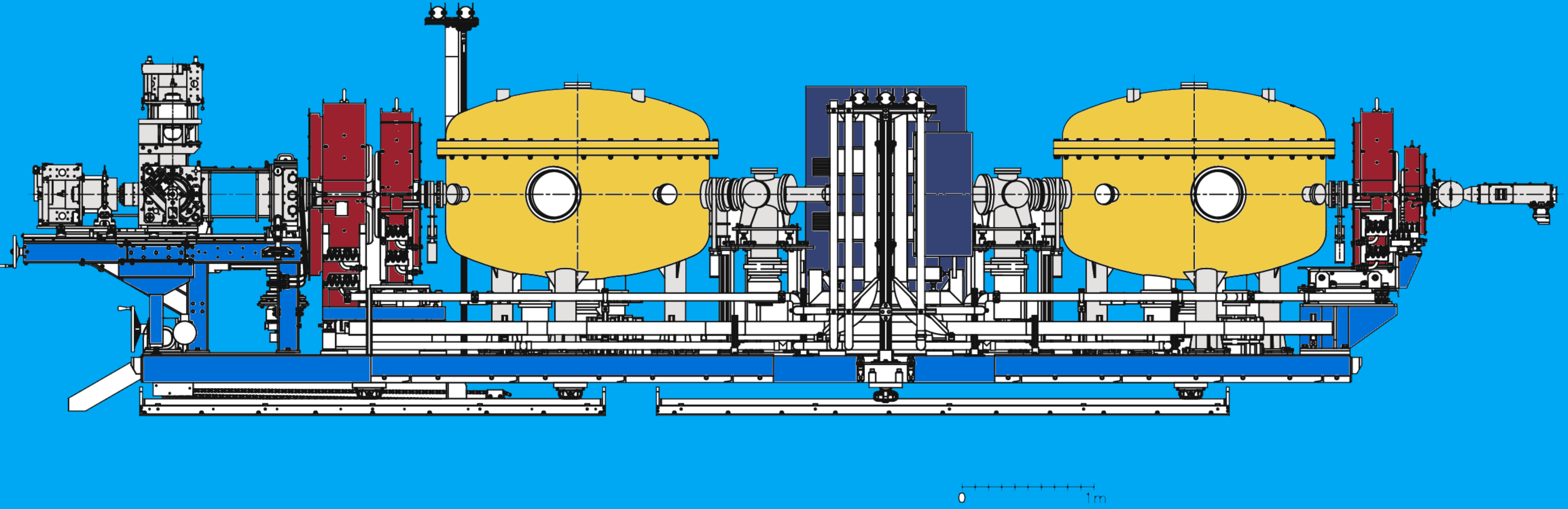

The Electro-Magnetic Mass Analyzer (EMMA)

PGAC

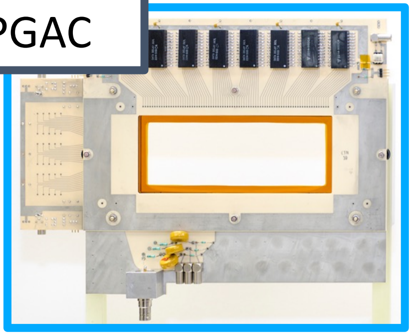

Ion Chamber

Ion-implanted Silicon

Angular Acceptance: ± 3.6° | Energy Acceptance: ±15% | m/q acceptance = ±3.3% | Rigidity limit: ~7q MeV

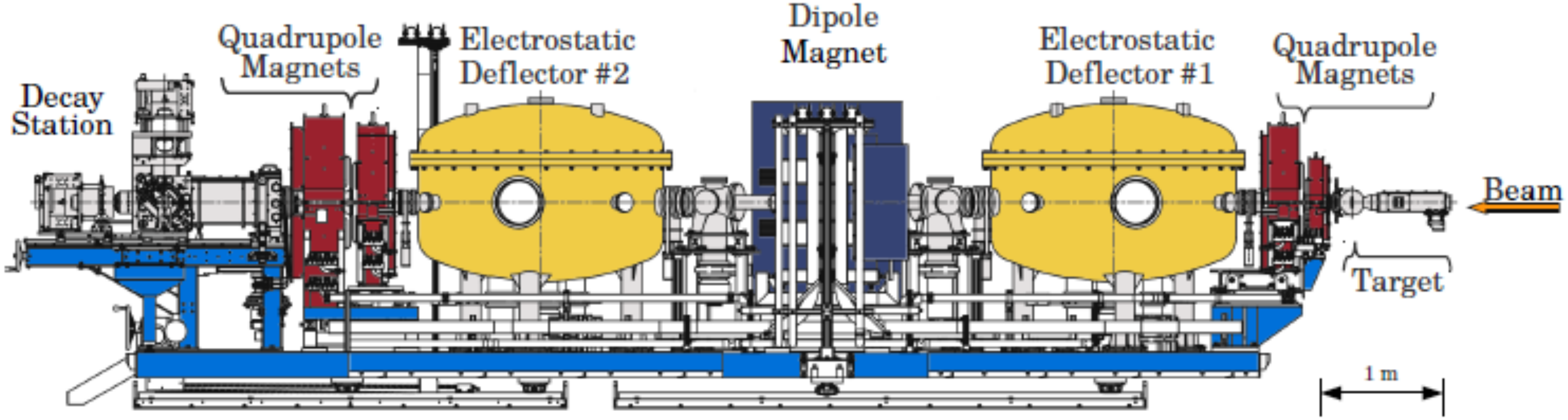

PGAC spectrum from Fusion Evap test run:

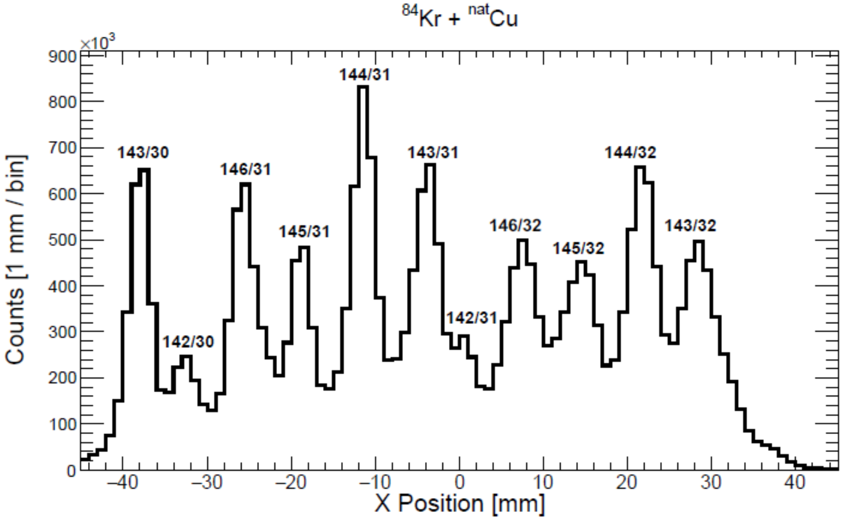

IC PID plot from ^{17}O experiment:

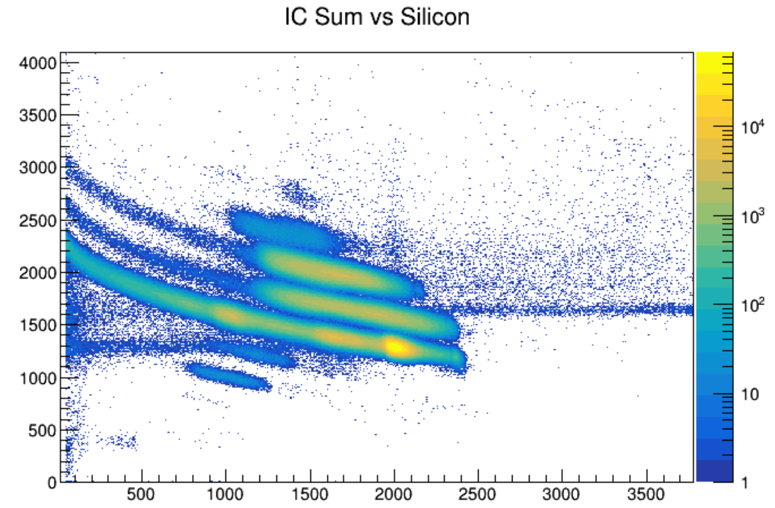

[1] B. Davids, M. Williams, *et al.*, *NIMA* ***930***, 191-195 (2019).

.

Beam suppression in EMMA

Need to use EMMA's slit systems to improve beam suppression.

- Suppression factor of slits alone was measured ~5 x10^4 with no cuts on the data
- Together with gate on Time-of-Flight total suppression up to ~10^{10} can be achieved


Focal plane slits

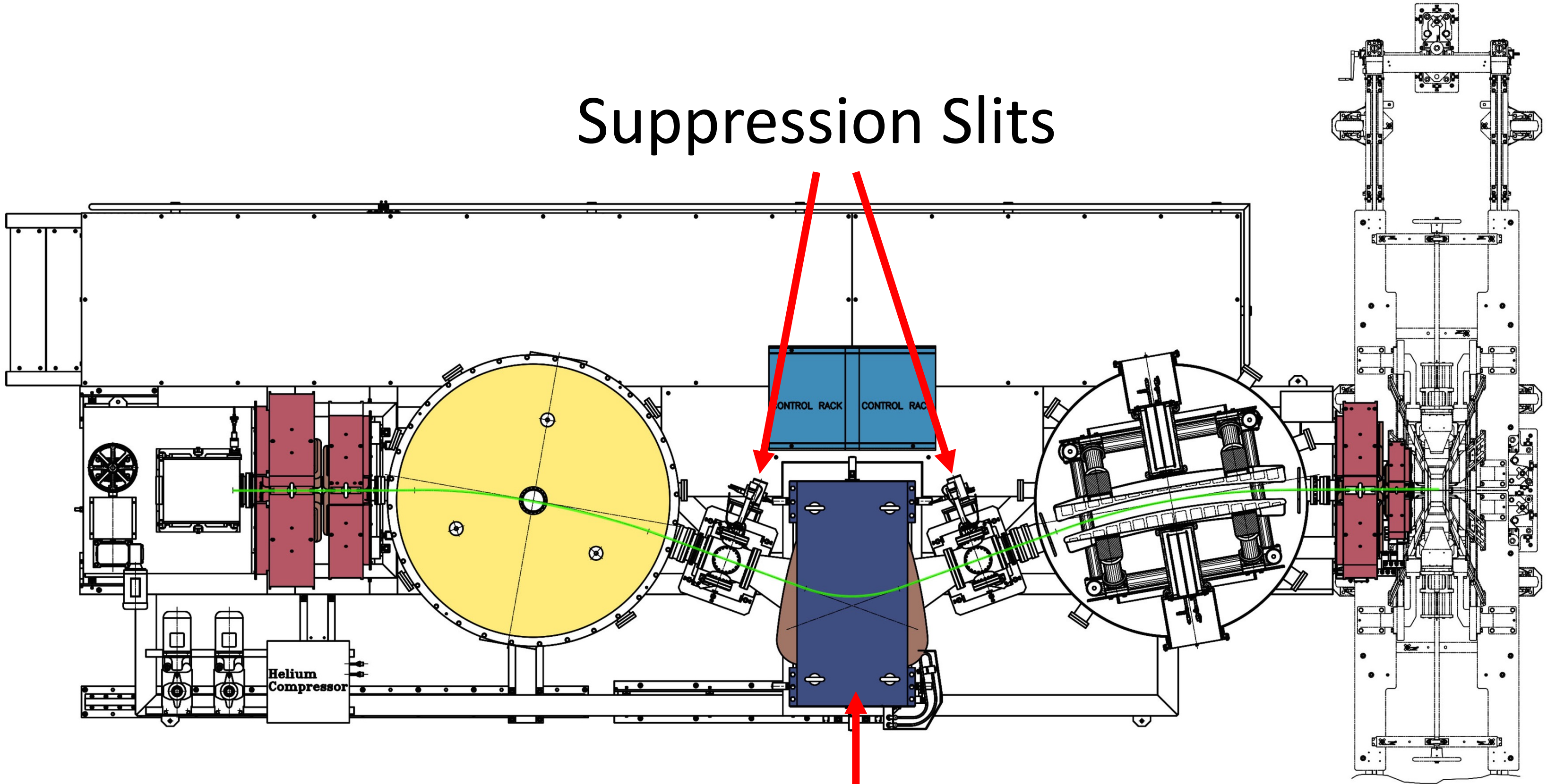

TIGRESS γ-detection array

- 12 Clover detectors with 8 centered at 90° and 4 at 135°
- segmented outer contacts for improved Doppler correction for spectroscopy after in-beam reactions
- 4 crystals in a common cryostat
- BGO Compton suppressor shields, reconfigurable in situ

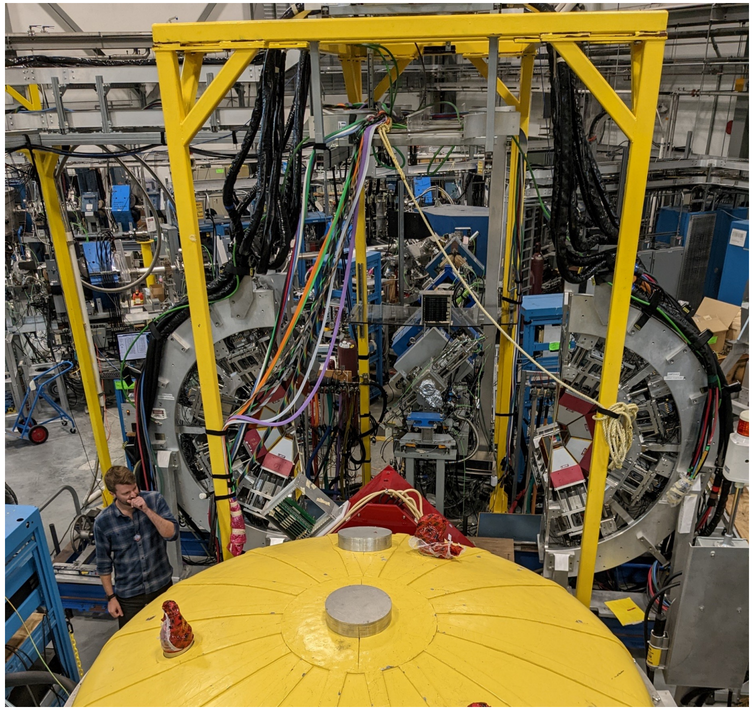

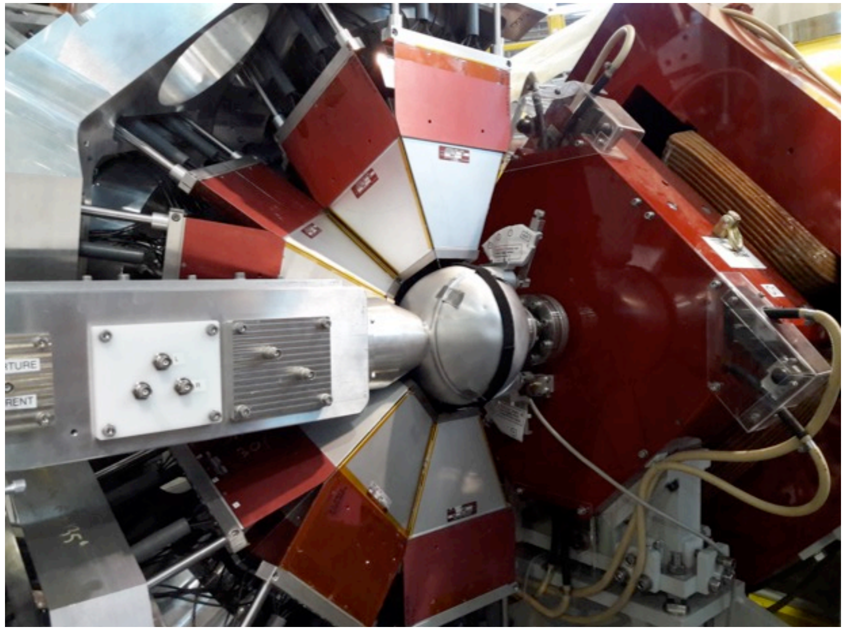

Studying the weak r-process with EMMA+TIGRESS

(α,n) reactions on isotopes of Kr, Rb and Sr are identified as particularly important for determining weak r-process abundance signatures.

Currently there is a lack of (α,n) cross-section data in this mass region, so all predictions rely on statistical model calculations, which carry large uncertainties (> x10).

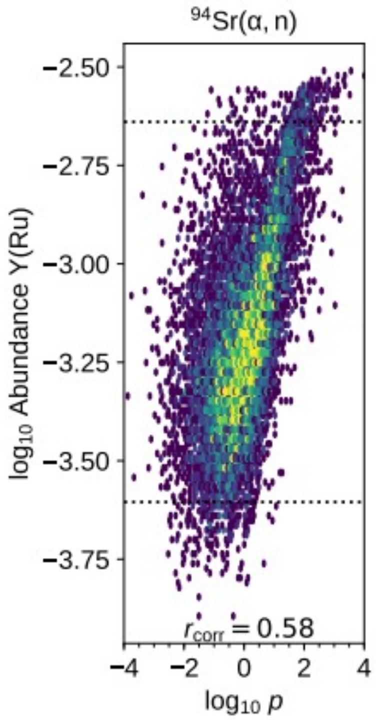

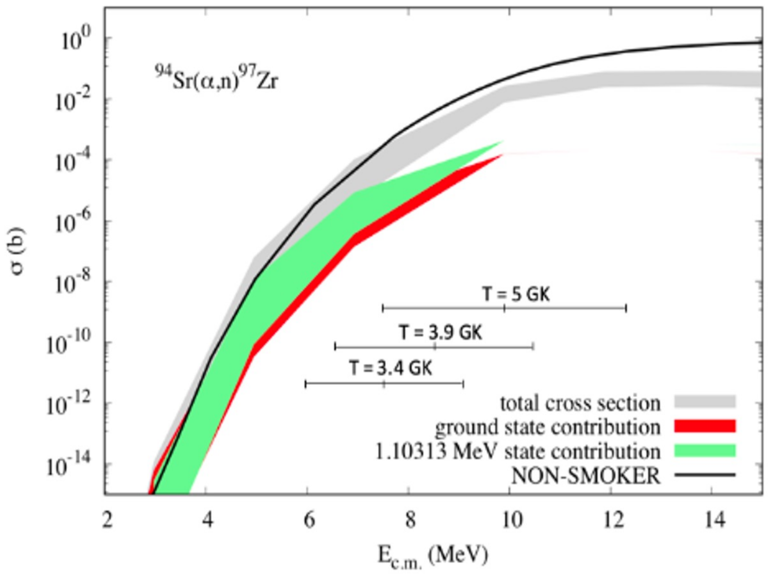

How to make a target from an inert gas?

- Typical options include gas targets and implanted foils
- Advances in materials science provides new options: Magnetron-sputtered silicon thin-films formed in a helium plasma environment.

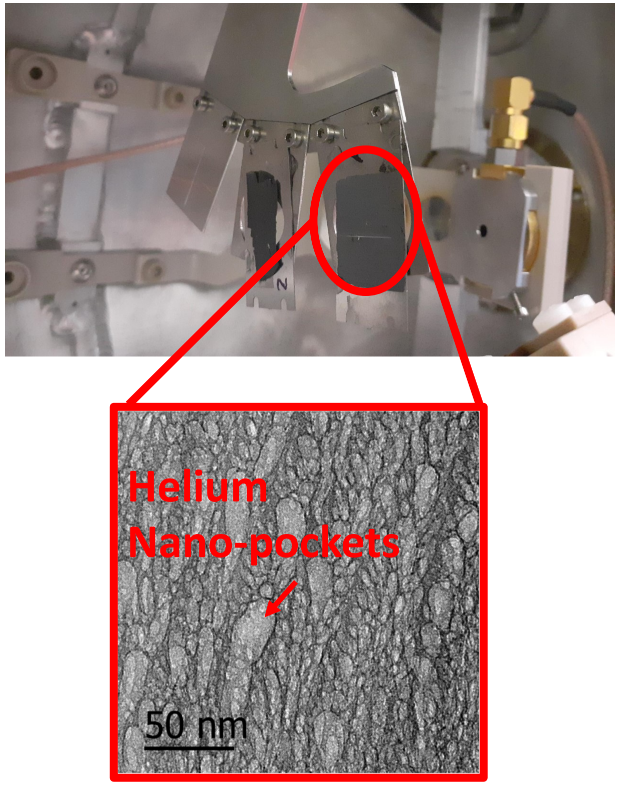

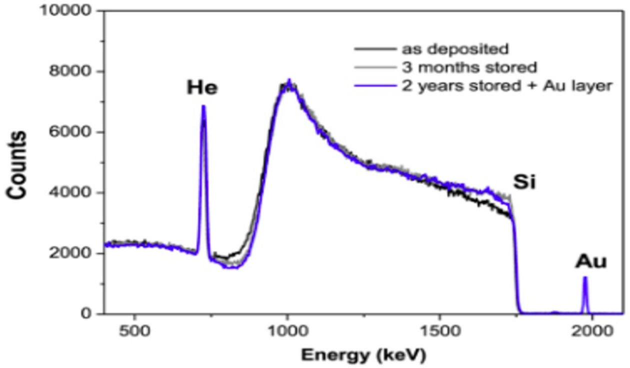

- ✓ High He density
- ✓ Homogeneous distribution.
- ✓ Content stable in storage and in beam.
- ✓ Compact with no expensive infrastructure.

[1] J. Bliss *et al.,* Phys. Rev. C **101**, 055807 (2020).
[2] V. Godinho *et al.*, ACS Omega 1,1229– 1238 (2016)

Slide from Matthew Williams

Measurement of $^{86}Kr(\alpha,n)^{89}Sr$

Two measurements were performed of $^{86}Kr(\alpha,n)^{89}Sr$ at 265 and 240 MeV bombarding energies
In both measurements a gold degrader foil was used, since the recoils would otherwise be too energetic to bend.

November 2021: Si:He targets were self-supported with a 2µm Gold degrader mounted ~10 cm downstream.

- Pro: little influence of degrader on γ-ray background (coulex).
- Con: recoil angles entering EMMA not constrained to region where EMMA's acceptances are known ($\pm 3^o$)

August 2022: Si:He targets were deposited directly onto a 4µm gold degrader foil.

- Pro: can use 3° aperture to define maximum recoil angle entering EMMA.
- Con: Introduces γ-ray background from coulex (not an issue for this particular experiment) also potential for Doppler broadening of some lines of interest (not yet confirmed).

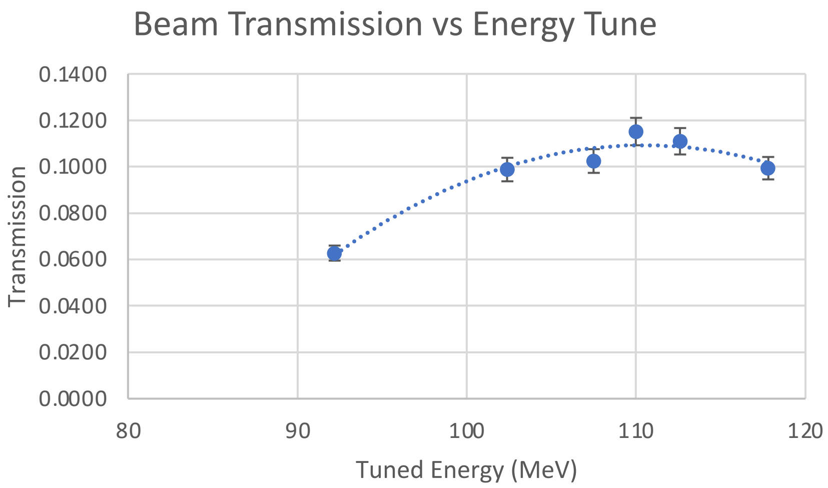

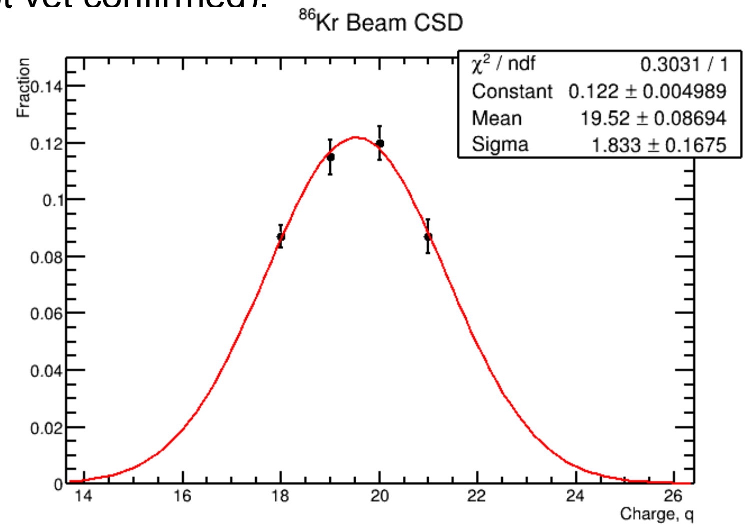

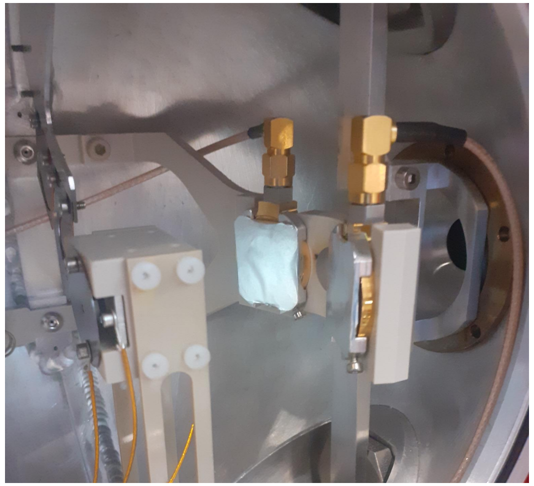

Transmission through EMMA was measured for different energy tunes and charge states to find optimum settings. Compare attenuated beam rate on scintillator vs focal plane.

Beam normalisation & target content measured via 2 SSB detectors

Slide from Matthew Williams

Stable beam test measurement: $^{86}Kr(\alpha,n)^{89}Sr$

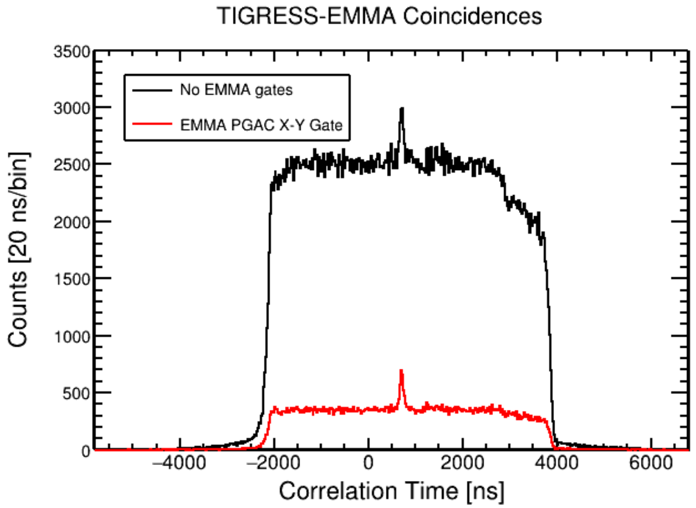

EMMA was tuned to A=89 (q=19+) 89.7 MeV recoils

- See clear peak in the timing signal between EMMA and TIGRESS events.
- The timing peak is also correlated with a well-focused A=89 (q=19+) peak seen in the focal plane X-position (dispersive direction).
- Able to pick-out clear ^{89}Sr γ-rays in coincidence with EMMA events gated on the PGAC spectrum. Can now use these γ-ray yields to constrain statistical model calculations.

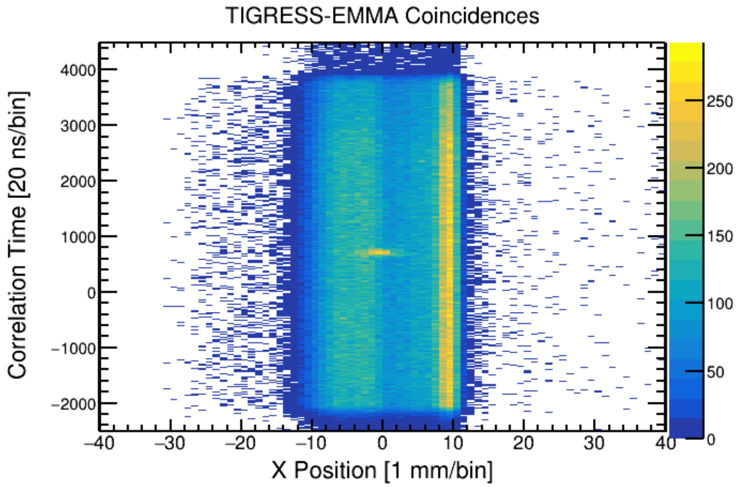

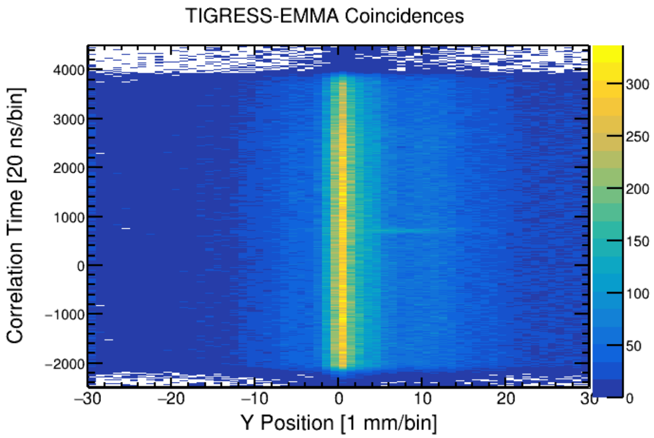

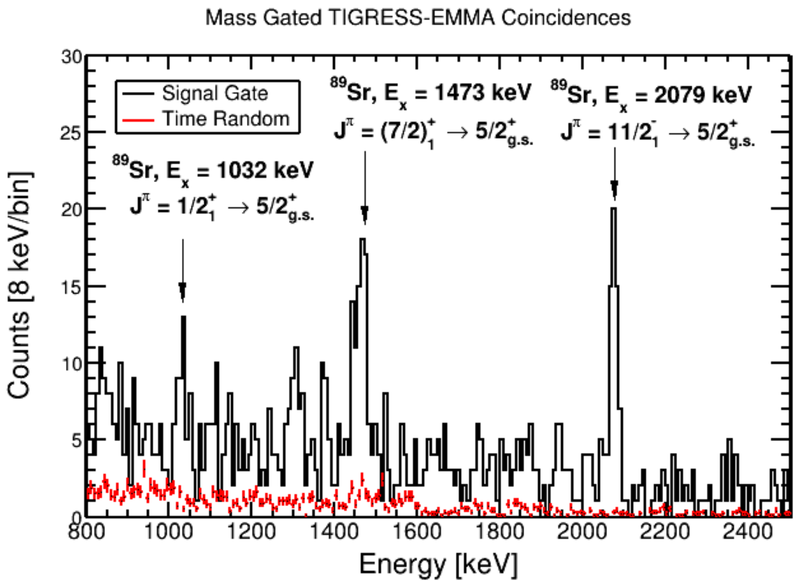

Measurements were successful with stable beam & targets clearly performed well!

Slide from Matthew Williams

Measurement of ^{83}Rb$(p,\gamma)^{84}$Sr

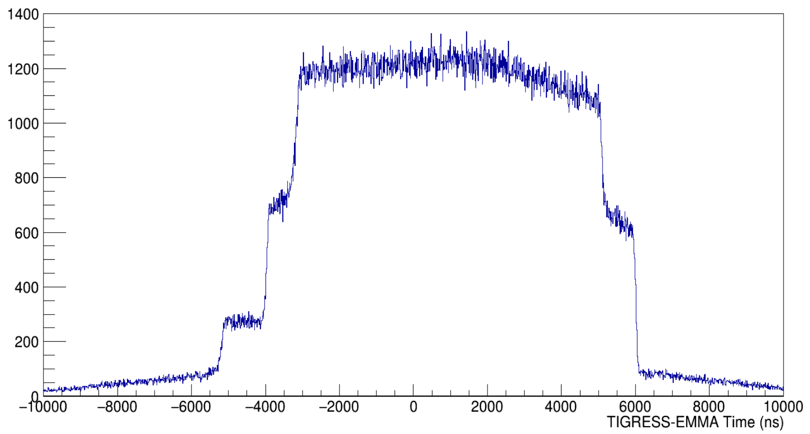

- Large background from ^{83}Sr contamination in the beam, which scatters onto EMMA's entrance aperture → obscures the timing peak!
- Plotting γ-ray energy vs the correlation time reveals signal of high energy γ-rays at the expected correlation time.
- Gating around the correlation peak reveals the transition from the first 2^+ to ground state transition in ^{84}Sr. (16 events above background)

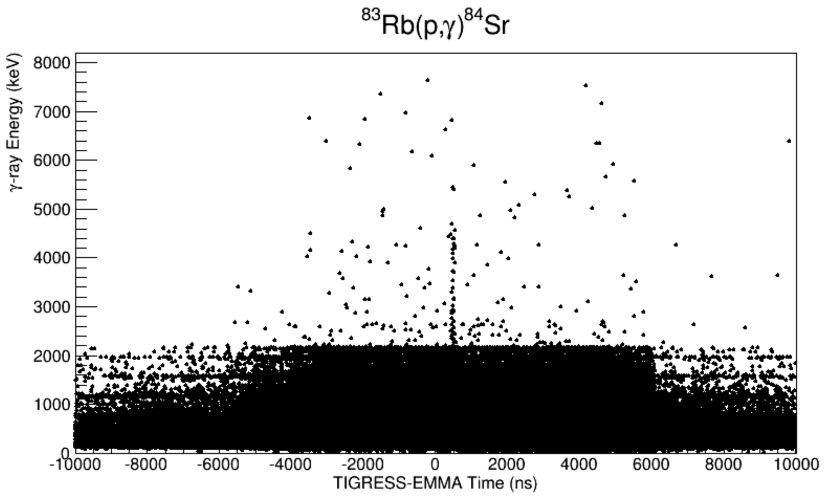

G. Lotay, S. Gillespie, M. Williams, et al., Phys. Rev. Lett. **127**, 1127

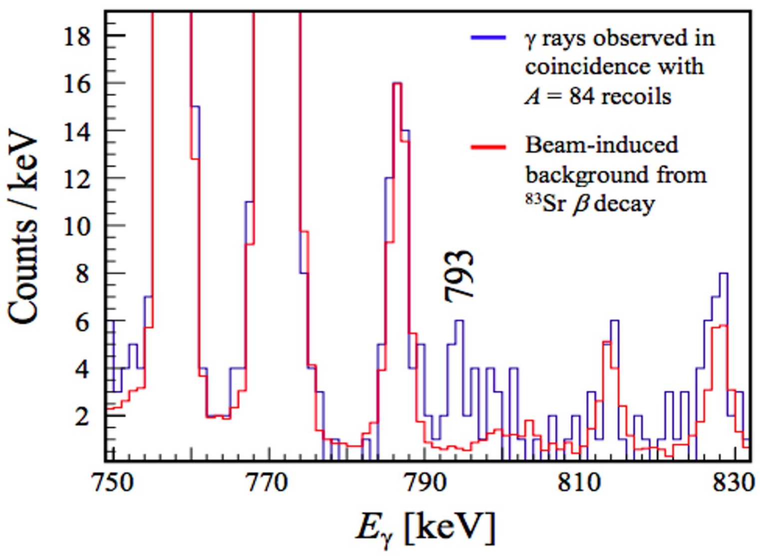

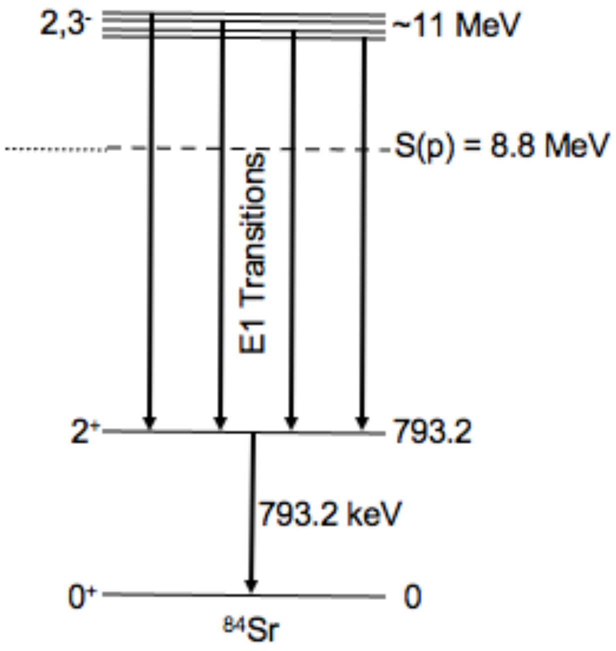

Slide from Matthew Williams

First measurement of a p-process reaction with a radioactive beam

Partial cross-section is converted to the full reaction cross section using γ-cascade models (included in the SMARAGD code), which predict 71 ± 10% of (p,γ) reactions result in a $2^+ \rightarrow 0^+$(g.s.) decay.

Total cross sections are approximately 4x smaller than predicted by Hauser-Feshbach models

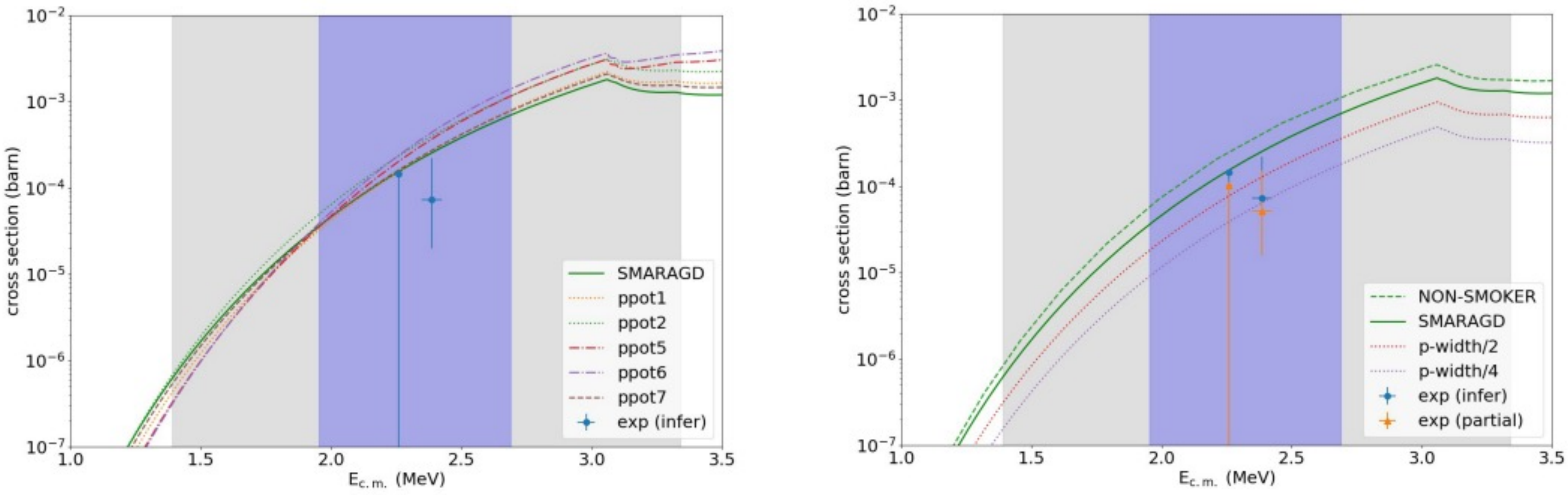

G. Lotay, S. Gillespie, M. Williams, *et al., Phys. Rev. Lett.* **127**, 112701 (2021).

M. Williams, *et al., Phys. Rev. C* **107**, 035803 (2023).

Statistical modeling by T. Rauscher

Slide from Matthew Williams

Astrophysical impact of ^{83}Rb$(p,\gamma)^{84}$Sr measurement

Investigated for both Type II and Type Ia supernovae explosions

- Lower ^{83}Rb$(p,\gamma)^{84}$Sr cross-section leads to less efficient destruction of the ^{84}Sr p-nucleus in supernovae, raising its production factor.
- The total uncertainty in ^{84}Sr production is reduced by a factor of 2 from previous sensitivity study.
- Uncertainties represent the combined effect of all reaction rates variations – not just ^{83}Rb$(p,\gamma)^{84}$Sr.
- Abundance enhancement not sufficient to explain enhanced ^{84}Sr seen in Allende Meteorite but could relieve tension – full GCE simulations required!

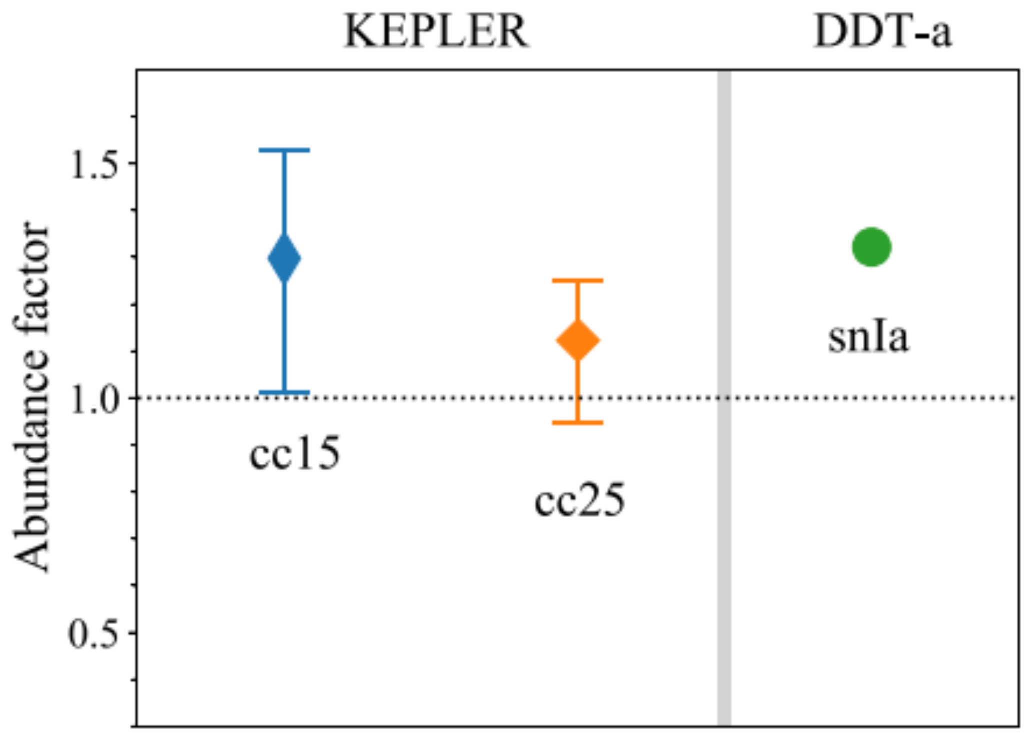

15 $M_\odot$ CCSNe = +30 %
25 $M_\odot$ CCSNe = +12 %
Type 1a SNe = +32 %

Astrophysical modeling by N. Nishimura

M. Williams, *et al., Phys. Rev. C* **107**, 035803 (2023).

New target chamber SHARC-II for EMMA & TIGRESS

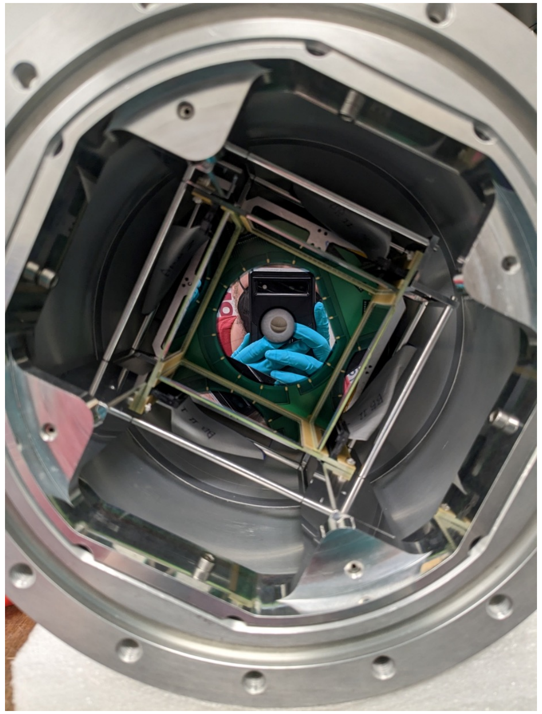

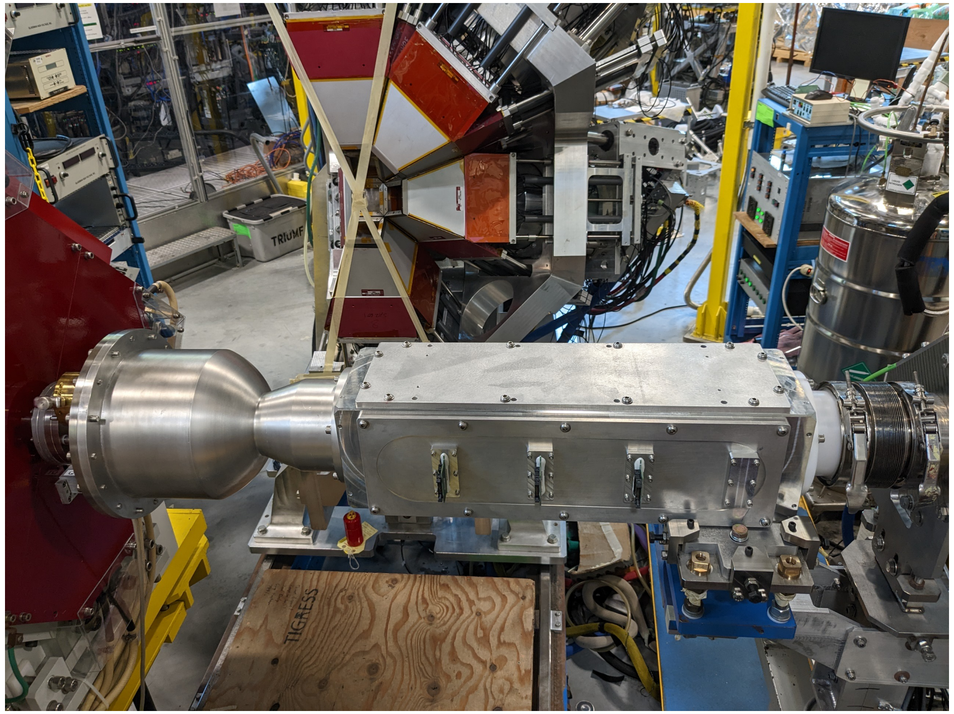

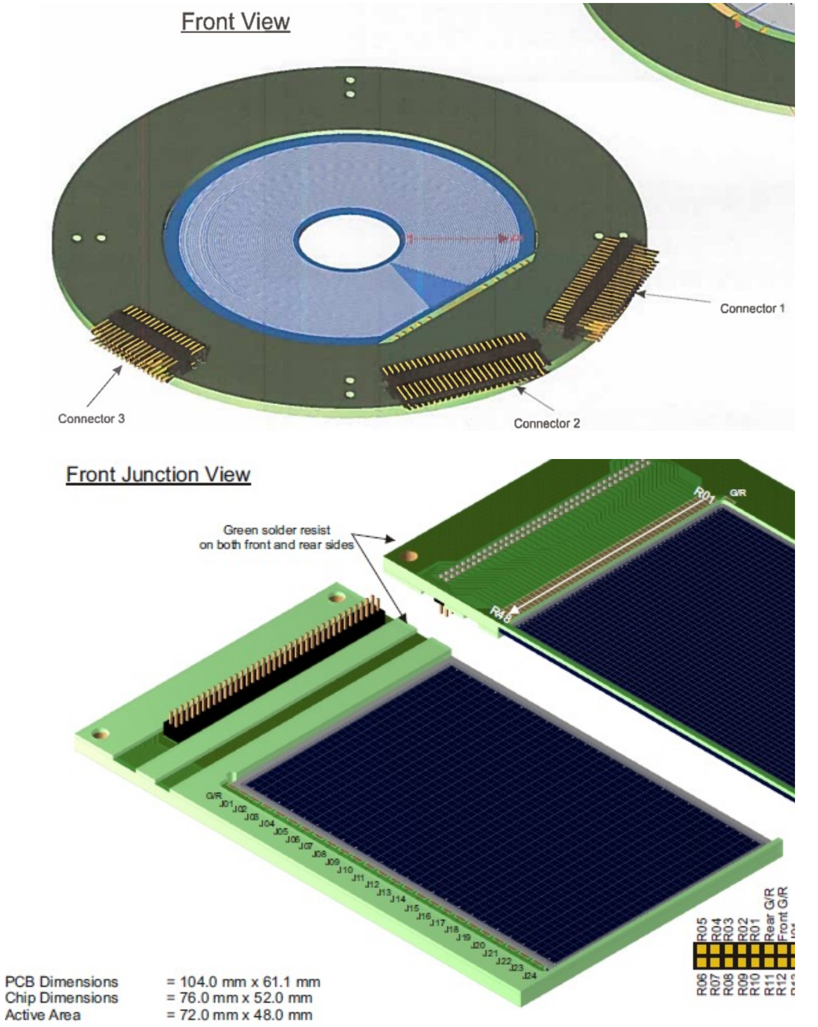

- Upgrade of SHARC target chamber to connect it to EMMA
- Designed by C. Diget et al., J. Instrum. 6, P02005 (2011)
- 6 DSSSD detectors to cover angular range of:
  10° – 28° ~ 100° – 140° 146° – 172°

Test of new target chamber SHARC-II with EMMA & TIGRESS

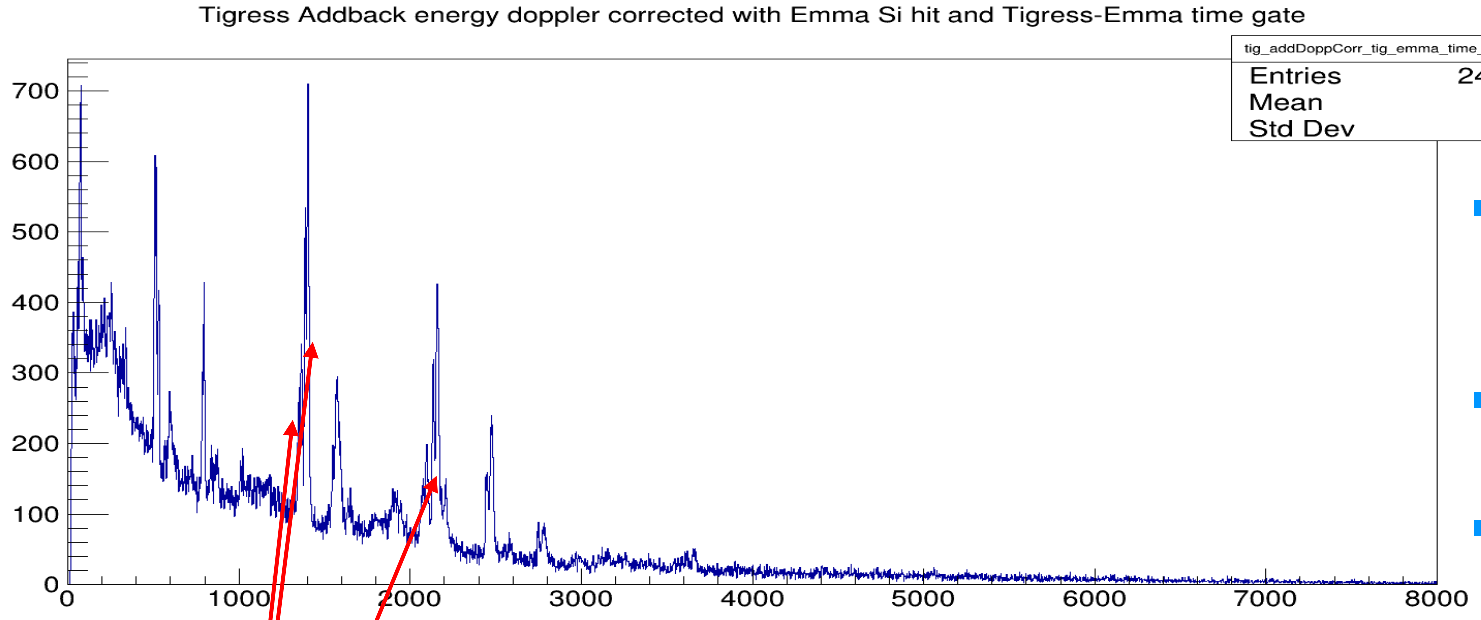

- Tested with ^{36}Ar 7+ beam impinging on 3 MeV/u on CD_2 target 300μg/cm²
- Simultaneous measurement of ^{36}Ar(d,p)^{37}Ar and ^{36}Ar(d,n)^{37}K
- Different gate conditions reveal (d,p) and (d,n) reactions

TABLE 1

Absolute transition strengths G_{lj} from ^{36}Ar(d, n)^{37}K and ^{36}Ar(d, n)^{37}K

$^{37}K^*$ [a] (MeV)	J_f^π [a]	l [b]	G_{lj} [b] (d, n) E_d = 5.6 MeV	G_{lj} [c] (τ, d) E_τ = 11.8 MeV
0.0	$\frac{3}{2}^+$	2	2.0	1.4
1.368	($\frac{1}{2}^+$)	0	0.20	
1.380	$\frac{7}{2}^-$	3	4.6	5.12
2.169	($\frac{3}{2}^-$)	1	1.6	1.32
2.750	$\frac{5}{2}^+$	(2)	0.10	
3.083	($\frac{5}{2}^-$)	(3)	0.4	
3.311	$\frac{3}{2}^-$	1	0.4	

[a]) From ref. [8]).
[b]) From present experiment. The uncertainty in absolute magnitude of the G_{lj} is about 30 %.
[c]) Obtained by re-analyzing the data of ref. [1]) with DWBA using the τ-potential of ref. [15]), and the d-potential set 1 of ref. [11]). No NL corrections were applied, and N = 4.4 was used.

M. HAGEN, U. JANETZKI and K.-H. MAIER Nuclear Physics A152 (1970) 404--418

Louis Wagner

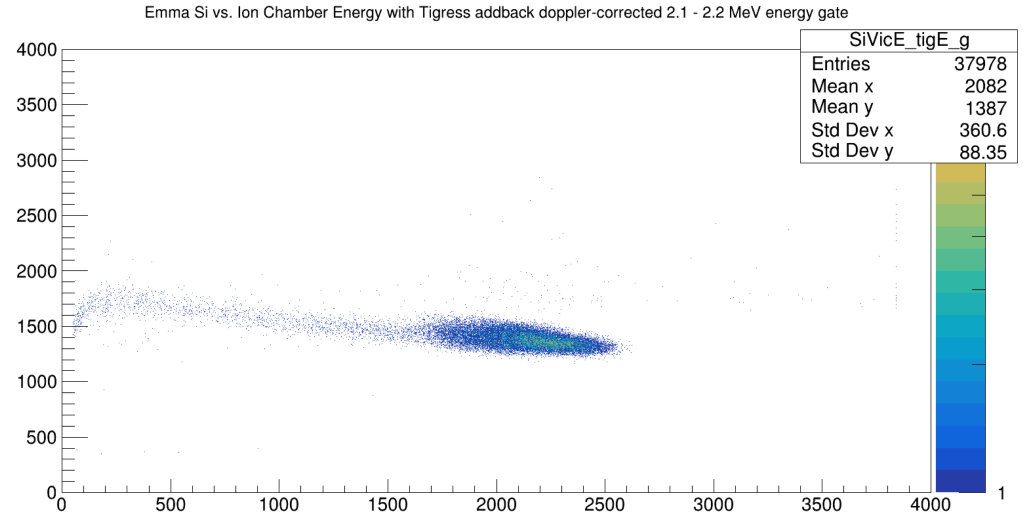

SUMMARY / OUTLOOK

- Transfer reactions critical for many astrophysical processes/sites but very challenging to measure
- Recoil mass spectrometer very specific device to solve issue (primarily for RIB)
- Techniques well developed for all conditions: low cross section, beam contaminants
- Recoil Separation needed to making *pioneering* measurements, i.e. first direct measurements of p-process reaction with radioactive beam
- Can contribute to precision measurements of stable reactions as well, complementary to normal kinematics

- Upcoming EMMA experiment in August:
  $^{86}Kr(\alpha,n)^{89}Sr$ and $^{94}Sr(\alpha,n)^{97}Zr$ (Part III) for weak r-process
- SHARC-II chamber allows transfer reaction measurement with full information on reaction products (light particle, gamma & recoil)
- Decay station for studying recoil decay will be assembled over the next year

TRIUMF

My thanks to Barry Davids (TRIUMF) & Matthew Williams (Uni of Surry) for slides and to all my collaborators at EMMA & TIGRESS!

Thank you
Merci

www.triumf.ca

Follow us **@TRIUMFLab**

Discovery, accelerated

Backup Slides

Inverse Kinematics

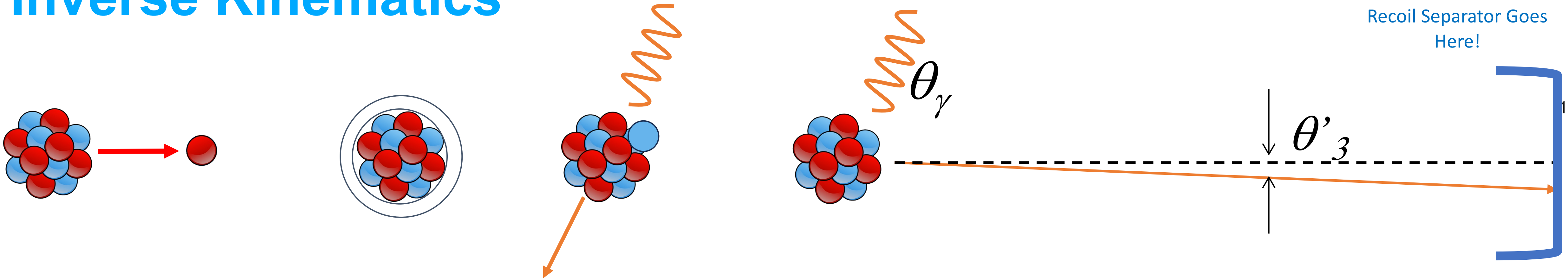

- **Maximum** possible **recoil angle** when E_γ is maximized for $E_\gamma = Q + E_{c.m.}$
- AND emission perpendicular to beam axis **($\theta_\gamma = \pi/2$)**

$$\tan\theta'_{3,\max} \simeq \frac{Q+E}{\sqrt{2\frac{m_1}{m_2}(m_1+m_2)E}}$$

$$\frac{\Delta p'_3}{p'_3} \simeq \frac{E_{\gamma,\max}}{p'_1} \simeq \theta'_{3,\max}$$

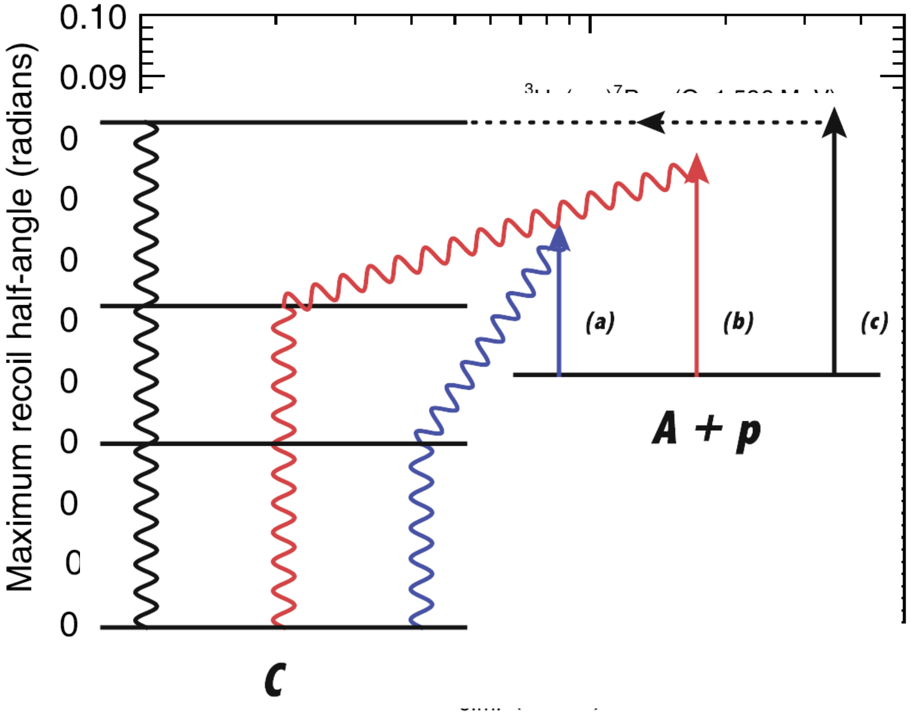

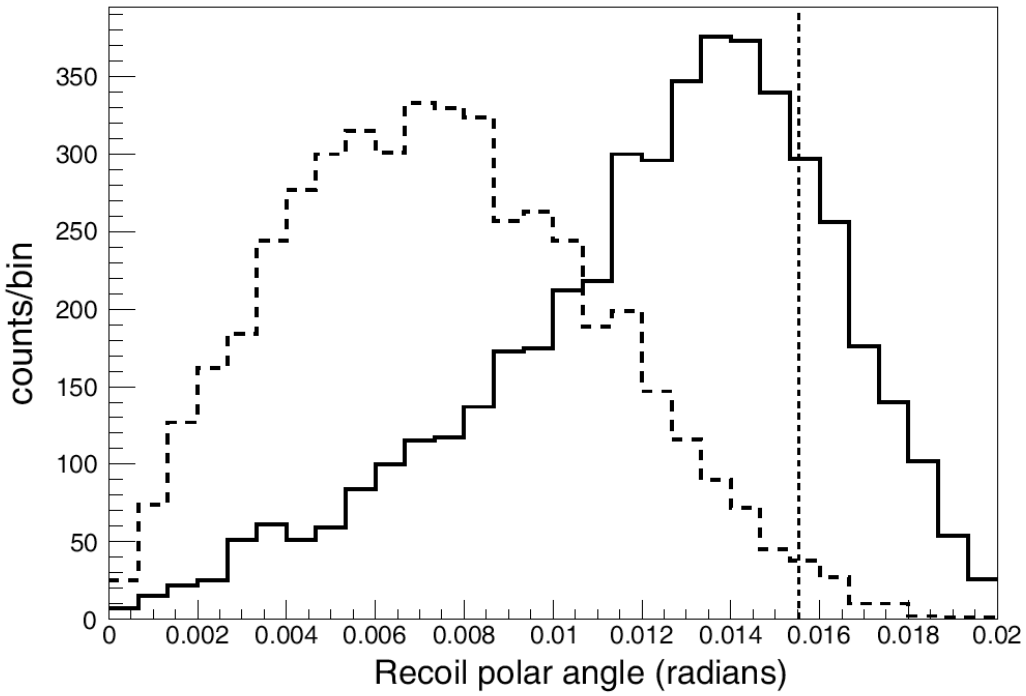

The Challenge

- In inverse kinematics we have:
- – Beam that did not interact
- – Recoil with, in average, the same momentum as the beam
- – Recoil with an momentum/energy distribution
- – Recoil with an angular opening that is larger than that of the beam
- – Beam and recoil with various charge states

Difficult to detect the recoils right after the target

Recoil separators are devices which separate nuclear reaction products (recoils) leaving a target from the unreacted beam particles.

Inverse Kinematics

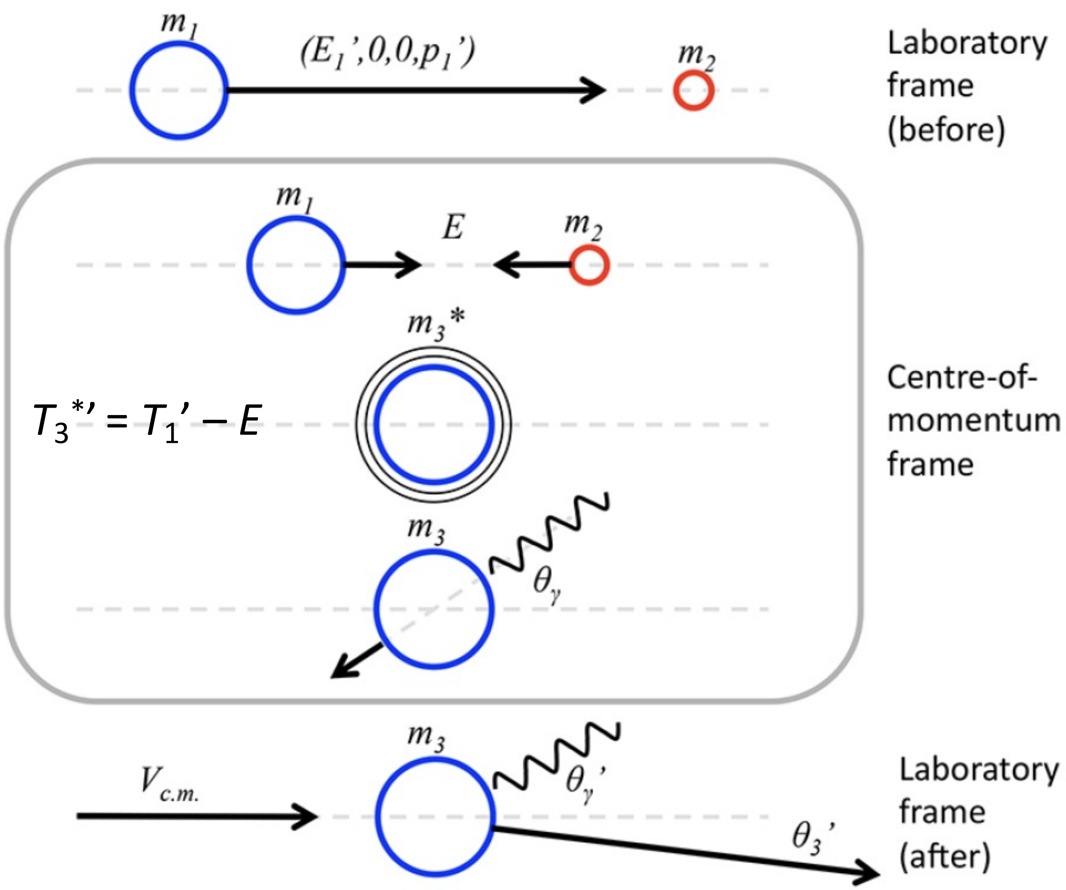

- Necessity due to not being able to make short-lived radioactive targets
- Detect recoiling product nucleus: forward focused, 100% efficiency
- Becomes problem of separating **rare** reaction products from **abundant** beam
  → zero-degree electromagnetic separator
- Additional advantages:
  - Target either H_2 or He: usually gaseous → windowless (jet,extended), purified etc…
  - Still detect gamma rays (tag)
  - Particle ID on reaction products

Two-Body Kinematics Calculator and Plotter

http://skisickness.com/2020/02/kinematics/

Angular distribution of recoils

From: PoS(ENAS 6)058

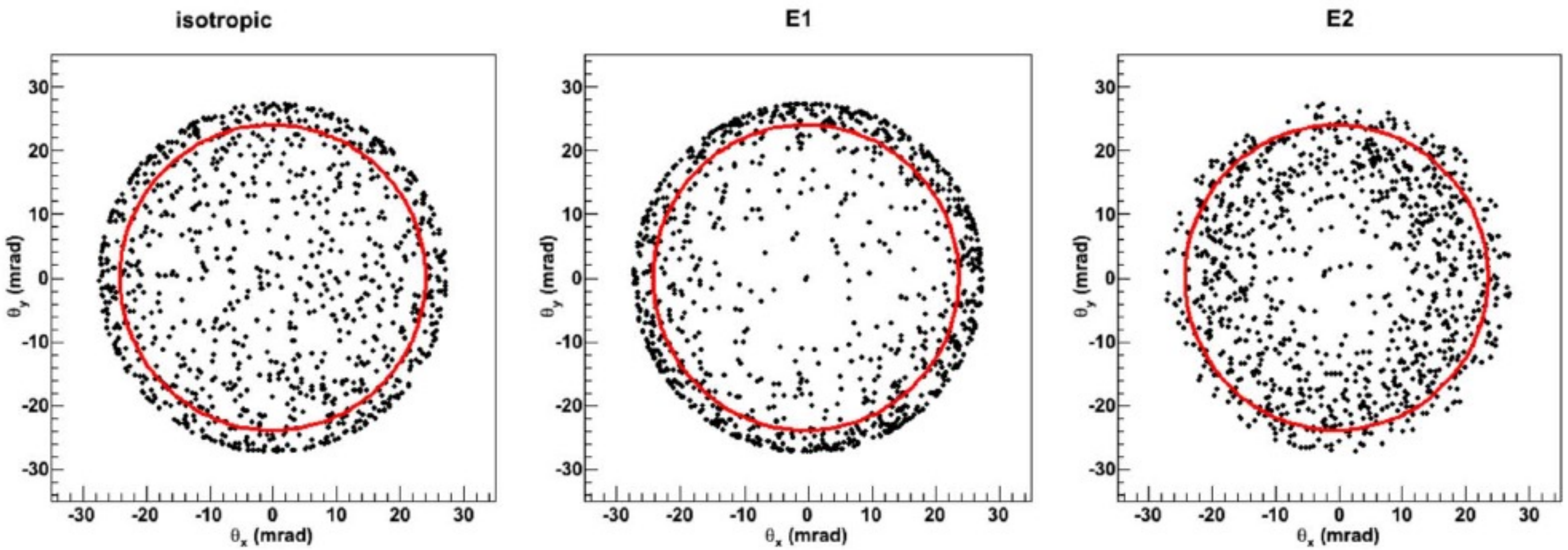

Figure 1 Distribution of recoils in the θ_x, θ_y space for $^{12}C(\alpha,\gamma)^{16}O$ ground state transition at E = 1.0 MeV. For different γ-ray angular distributions. Left: isotropic. Center: $\sin^2\theta$. Right: $\sin^2\theta\cos^2\theta$. For reference, a circle shows an angular acceptance of 24 mrad. See text for details.

For absolute cross section, full transmission of the selected charge state is needed

Example from FMA to study $^{13}C(p,\gamma)^{14}N$ and $^{18}O(p,\gamma)^{19}F$ and $^{18}F(p,\gamma)^{19}Ne$ but limited in transmission